World Academy of Science, Engineering and Technology
International Journal of Materials and Metallurgical Engineering
Vol:12, No:10, 2018

Determining Full Stage Creep Properties from Miniature Specimen Creep Test

W. Sun, W. Wen, J. Lu, A. A. Becker

Open Science Index, Materials and Metallurgical Engineering Vol:12, No:10, 2018 publications.waset.org/10009661/pdf

Abstract**—**In this work, methods for determining creep properties which can be used to represent the full life until failure from miniature specimen creep tests based on analytical solutions are presented. Examples used to demonstrate the application of the methods include a miniature rectangular thin beam specimen creep test under three-point bending and a miniature two-material tensile specimen creep test subjected to a steady load. Mathematical expressions for deflection and creep strain rate of the two specimens were presented for the Kachanov-Rabotnov creep damage model. On this basis, an inverse procedure was developed which has potential applications for deriving the full life creep damage constitutive properties from a very small volume of material, in particular, for various microstructure constitutive regions, e.g. within heat-affected zones of power plant pipe weldments. Further work on validation and improvement of the method is addressed.

Keywords**—**Creep damage property, analytical solutions, inverse approach, miniature specimen test.

NOMENCLATURE

A	constant in Kachanov equations or cross-section area
$B, n, m, \alpha, \phi, \chi$	constants in Kachanov equations
b, d	cross-section dimensions
$D, \dot{D}$	damage and damage rate
E	Young's Modulus
h_1, h_2	thicknesses
I_n	n^{th} moment of area of bending (steady-state creep)
$K, \dot{K}$	curvature and curvature rate
L	length
M	bending moment
P	loading force
$S_1, S_2,$	cross-section areas
t	time
w	strain energy density
W_{ex}, W_{in}	total external work and total internal strain energy
x, y	Cartesian coordinates
$\varepsilon, \varepsilon^c, \dot{\varepsilon}^c$	strain, creep strain and creep strain rate, respectively
$\sigma, \sigma_i, \sigma_{eq}, , \sigma_r$	Stress, maximum principle stress, equivalent stress and rupture stress, respectively
$\Delta, \dot{\Delta}$	displacement and displacement rate

W. Sun is a Professor in the Department of Mechanical, Materials and Manufacturing Engineering at University of Nottingham, UK (phone: +441159513809; e-mail:w.sun@nottingham.ac.uk).

W. Wen is a PhD researcher and A. A. Becker is a Professor in the Department of Mechanical, Materials and Manufacturing Engineering at University of Nottingham, UK (e-mail: wu.wen@nottingham.ac.uk, a.a.becker@nottingham.ac.uk).

J. Lu is an Assistant Professor in the Department of Mechanical, Material and Manufacturing Engineering at University of Nottingham, Ningbo, China (e-mail: Jiawa.Lu@nottingham.edu.cn).

I. INTRODUCTION

HIGH temperature thermal systems such as power plant steam piping work and gas turbines, chemical plant pressure vessels, aero-engine combustion structures, etc., may fail due to long term creep, fatigue and cyclic viscous-plasticity. During the service life under elevated temperature, the material and components used in these thermal systems will degrade and the creep strength of the material will significantly reduce. Non-destructive testing and small specimen test techniques have been employed to sample and test the material. For this reason, various small-sized, miniature specimen test methods have been developed [1] and used to assist in condition minoring and life management programs [2], [3]. The miniature test samples used for testing may be produced by scooping techniques, which remove small pieces of materials from in-serve component surfaces. One of important issues on the development of miniature specimen test techniques is the requirement for new test methods, which are suitable to test, for example, thin structures, such as coating or coating-substrate systems.

Small specimen creep testing has become increasingly attractive for power plant applications because some power plant components are now operating beyond their original design life, and economic, "non-invasive" and reliable testing techniques are required when performing remaining life evaluations. Data from small volumes of materials have a direct input into remaining life and ranking studies, thereby improving the confidence of plant/component life prediction and managing the potential risk [4]-[6]. Such data can also be used to generate creep constitutive laws for weld materials and for local heated-affected zone structures generated during the welding process [7].

The main small specimen types that are used to obtain creep properties include the conventional sub-size uniaxial specimens [8] and several specialised miniature specimen types including: the impression specimen [9], the small punch specimen [10], the small ring specimen [11], and the small tensile two bar specimen [12], see Fig. 1. One of the unique advantages the small punch creep test has is that one of the specimen dimensions (the thickness) is very small (~ 0.5 mm), however, up to date, there are no universally accepted conversion

techniques available for data interpretation, due to its complicated deformation and failure mechanisms [10], [13]. Previous research has also been carried out on miniaturised beam/thin plate bending specimen types [14], [15].

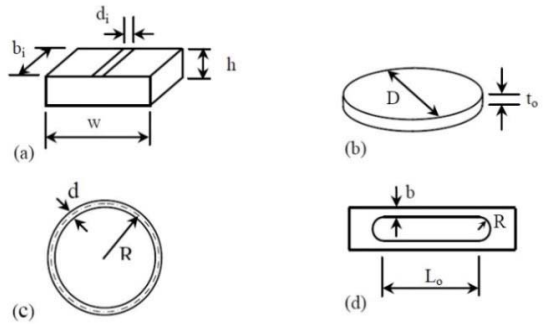


Fig. 1 Commonly used miniature creep test specimens: (a) Impression; (b) Small punch; (c) Small ring; and (d) Small two bar

Impression and ring type creep tests can only produce steady-state creep data. The two-bar specimen can produce the full stage creep curves, but it is difficult to make it very thin due to the pin loading nature, and to ensure that the two bars will fail at the same time. Currently, there is an important need for determining the elastic-plastic and creep properties from thin films and coatings. In this work, methods for determining creep damage properties using the miniature thin beam bending and two-material thin plate tensile creep tests which can be used to represent the full life until failure on analytical solutions and numerical modelling using an inverse approach are presented.

II. Creep Damage Constitutive Equations

The multiaxial form of the Kachanov-Rabotnov [16], [17] creep damage model is as following:

$$\dot{\varepsilon}_{ij}^{c} = A\frac{3}{2}\left(\frac{\sigma_{eq}}{1-D}\right)^{n}\left(\frac{S_{ij}}{\sigma_{eq}}\right)t^{m} \tag{1}$$

$$\dot{D} = B\frac{\sigma_r^{\chi}}{(1-D)^{\phi}}\,t^{m} \tag{2}$$

where $A, B, m, n,\ \phi$ and χ are material constants, and t is the time. σ_r is a rupture stress, defined as:

$$\sigma_r = \alpha\sigma_1 + (1-\alpha)\sigma_{eq} \tag{3}$$

where σ_1 and σ_{eq} are the maximum principal and von Mises equivalent stresses, respectively, and α is a material constant which is related to the tri-axial stress state of the material. The model has a good capability of representing the full stage (primary, secondary and tertiary) creep deformation until rupture. The uniaxial form of (1) and (2) are as follows:

$$\dot{\varepsilon}^{c} = A\left(\frac{\sigma}{1-D}\right)^{n}t^{m} \tag{4}$$

$$\dot{D} = B\frac{\sigma^{\chi}}{(1-D)^{\phi}}\,t^{m} \tag{5}$$

III. Analysis Of Small Bending And Two-Material Tensile Specimens

A. Three Point Bending Specimen

The geometry and load for the miniature three-point bending (TPB) specimen is shown in Fig. 2, where P is the applied point load, L is the length of the beam, and b and d are cross-sectional dimensions. Δ is the load direction creep displacement.

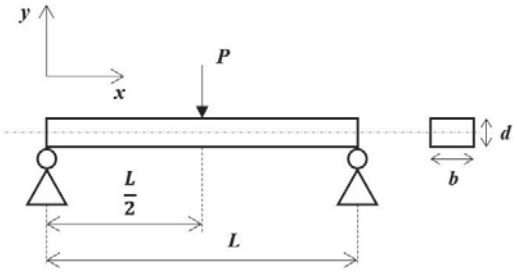


Fig. 2 Specimen in Three Point Bending.

The bending moment of the beam can be expressed as:

$$M = \int_A y\sigma dA \tag{6}$$

where y is the distance from the neutral axis and A is the cross-sectional area of the specimen. The strain compatibility of the beam by assuming the only strain changing over time is due to creep indicates that:

$$\dot{\varepsilon}^{c} = \dot{K}y \tag{7}$$

where K is the curvature of the beam ($\approx d^2y/dx^2$). Using (4) - (7) the stress distribution through the beam can be subsequently derived as:

$$\frac{\sigma}{1-D} = \frac{M|y|^{\frac{1}{n}}}{I_n}sgn(y) \tag{8}$$

where I_n is the n^{th} moment of inertia of a rectangular cross-section modified by the damage parameter:

$$I_n = \int_A |y|^{1+\frac{1}{n}}(1-D)dA \tag{9}$$

The deflection rate is calculated by the complementary strain energy method. The strain energy density w in a beam can be written as:

$$w = \frac{1}{2E}\sigma^2 + \int_0^t \sigma\dot{\varepsilon}^{c}\ dt \tag{10}$$

where E is the Young's Modulus of the beam. The total strain energy is expressed as:

$$W_{in} = \int_0^L \int_A w\, dAdx \tag{11}$$

On the other hand, the work done by the applied force at the centre of the beam is a function of its rate of change of vertical

Open Science Index, Materials and Metallurgical Engineering Vol:12, No:10, 2018 publications.waset.org/10009661/pdf

Open Science Index, Materials and Metallurgical Engineering Vol:12, No:10, 2018 publications.waset.org/10009661/pdf

displacement rate ($\dot{\Delta}$) and the force applied (P):

$$W_{ex} = \int_0^t P\,\dot{\Delta}\,dt \tag{12}$$

By balancing the work done by the external force and total internal strain energy gives,

$$P\dot{\Delta} = \int_0^L \int_A \sigma \dot{\varepsilon}^c\, dA dx \tag{13}$$

$$\dot{\Delta} = \frac{bA}{P} \int_0^L \int_d \frac{\sigma^{n+1}}{(1-D)^n} t^m\, dy\, dx \tag{14}$$

No closed form analytical solution could be obtained.

B. Tow-Material Tensile Specimen

A two-material tensile specimen is shown in Fig. 3. The two layers have equal length, L, equal width, and different thicknesses, h_1 and h_2, and therefore, different cross-sectional areas, S_1 and S_2. It is assumed that the properties of one of the materials are known (e.g. the substrate material properties for a coated system).

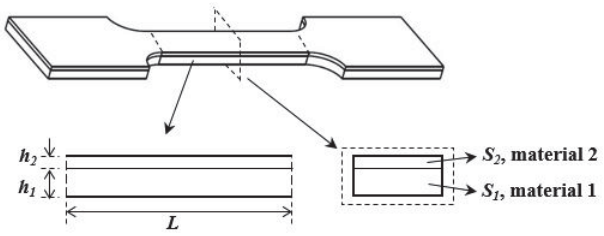


Fig. 3 A two-material tensile specimen

For material 1 shown in Fig. 3, the constitutive equations are (assuming m = 0):

$$\dot{\varepsilon}^c = A_1 \left(\frac{\sigma_1}{1-D_1}\right)^{n_1} \tag{15a}$$

$$\dot{D}_1 = B_1 \frac{\sigma_1 \chi_1}{(1-D_1)\phi_1} \tag{15b}$$

Since the creep properties of material 1 (A_1, n_1, B_1, χ_1, and ϕ_1) are known, the stress σ_1 can be determined from (16) by applying the experimentally determined minimum strain rate (MSR), $\dot{\varepsilon}^c{}_{min}$, for the steady-state creep, during which there is no creep damage, i.e. $D_1 = 0$:

$$\sigma_1 = \left(\frac{\dot{\varepsilon}^c{}_{min}}{A_1}\right)^{\frac{1}{n_1}} \tag{16}$$

By considering the equilibrium and compatibility, the stress in material 2 can be determined as follows:

$$\sigma_2 = \frac{P-\sigma_1 S_1}{S_2} = \frac{P-\left(\frac{\dot{\varepsilon}^c{}_{min}}{A_1}\right)^{\frac{1}{n_1}} S_1}{S_2} \tag{17}$$

The creep constitutive equations of material 2 are as follows:

$$\dot{\varepsilon}^c = A_2 \left(\frac{P-\left(\frac{\dot{\varepsilon}^c{}_{min}}{A_1}\right)^{\frac{1}{n_1}} S_1}{S_2(1-D_2)}\right)^{n_2} \tag{18a}$$

$$\dot{D}_2 = \frac{B_2}{(1-D_2)\phi_2} \left(\frac{P-\left(\frac{\dot{\varepsilon}^c{}_{min}}{A_1}\right)^{\frac{1}{n_1}} S_1}{S_2}\right)^{\chi_2} \tag{18b}$$

where A_2, n_2, B_2, χ_2, and ϕ_2 are the unknown creep constants of material 2, which can be determined numerically using (17), (18a) and (18b).

IV. Inverse Procedure

A. Three Point Bending

This method is developed and used to iteratively determine the creep properties based on the known displacement versus time curves at the beam centre. The idea is to fit the displacement curves against time obtained in TPB tests to the target objective data iteratively to find an array of unknown material constants q_i that fit a series of TPB virtue test data. The optimisation process is available in the toolbox of MATLAB by the function *lsqcurvefit*. It is conducted by minimising the difference between the predicted results $y_i = F(q_i, time)$ and virtue test data set $ydata$, based on a nonlinear least-squares algorithm [18].

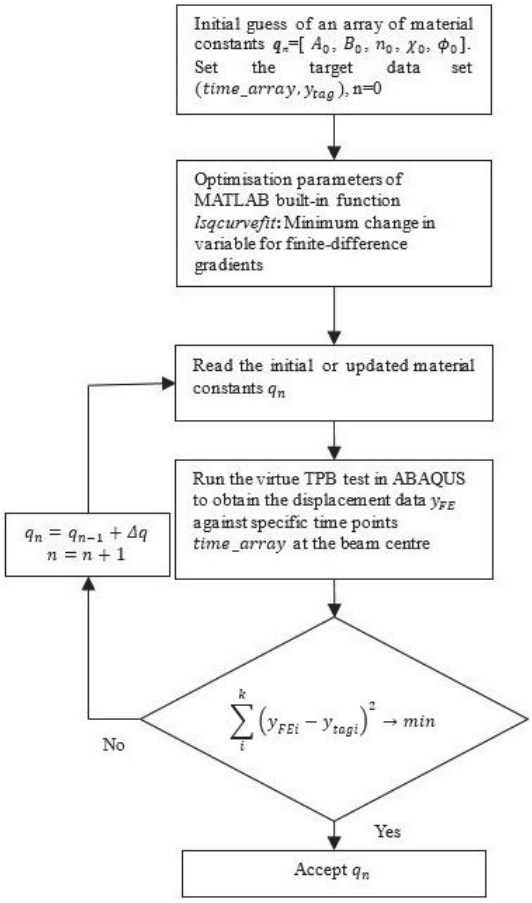


Fig. 4 Flowchart of the inverse method by MATLAB

Open Science Index, Materials and Metallurgical Engineering Vol:12, No:10, 2018 publications.waset.org/10009661/pdf

The predicted results are based on the estimated set of material constants q_i and the set of time points $time$. The virtue test data served as target data is given by $ydata = F(q, time)$. The flowchart is shown in Fig. 4.

TABLE I
CREEP AND DAMAGE PROPERTIES IN THE KACHANOV MODEL FOR THE P91 STEEL DERIVED FROM UNIAXIAL CREEP TESTS AT 650 ^{0}C (STRESS IN MPA, AND TIME IN HRS) [7]

Material	A	B	n	m	ϕ	χ
P91 Steel	1.092×10^{-20}	3.537×10^{-17}	8.462	-4.754×10^{-4}	7.346	6.789

To validate the mathematical expressions and the implementation codes for the inverse procedure, an finite element analysis (FEA) is performed for the problem using ABAQUS. The geometry of the specimen being modelled is set with $b = d = 1mm$, and $L = 12mm$. The length of the specimen is relatively large compared to its cross-section dimensions to ensure that the contribution of shear stress is negligible. Also, the beam is relatively narrow, allowing the valid assumption of plane stress conditions. The creep and damage properties used are taken from Table I. The displacement curves are displayed in Fig. 5 under a range of load P. From the curve, the effect of initial creep is negligible and hardly observed. There is clear steady state creep and tertiary creep. It can be seen that the FE and analytical results are practically the same.

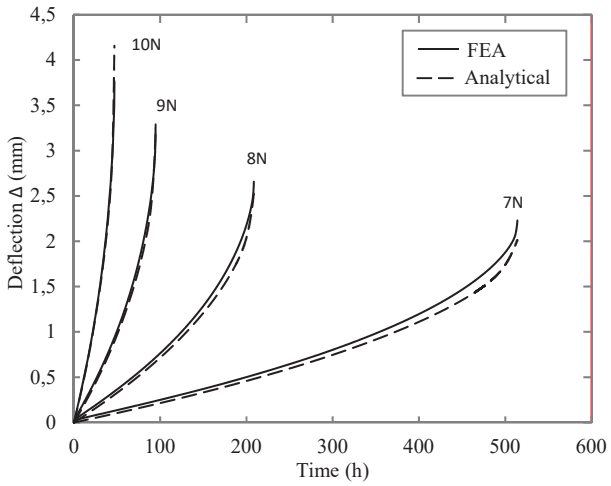


Fig. 5 Deflection curves obtained from the virtue TPB tests and the FE analysis for a range of loading

The next step is to demonstrate the applicability of the inverse procedure. An example of such demonstration is shown in Fig. 6, where the fitted deflections of beam center under a variety of loads using the optimised creep properties obtained from the inverse iteration are presented with the virtue test (theoretical experimental) curves. It can be seen that very good comparison is achieved.

B. Two-Material Tensile

An inverse method was also developed for the two-material case based on the forward analysis method presented in section III using a similar optimisation procedure as that for the TPB case. FEA can be avoided to save computing time since the results of the analytical solutions and FEA were very close, as shown in Fig. 7, regarding the evolutions of the strain, damage and stress. The material properties of the two materials used for the finite element (FE) modelling and the analytical calculation are presented in Table II. Fig. 8 shows a flowchart of the inverse algorithm. The experimental compound creep test results are supplied as the target values. The known material creep properties and an initial guess of the unknown material creep properties are supplied to the forward analysis method of the two-material system developed based on the Kachanov creep damage model (section III). A nonlinear optimisation algorithm is used to minimise the differences between the predicted compound creep responses and the experimental results until a set of optimised creep damage properties are obtained for the unknown material.

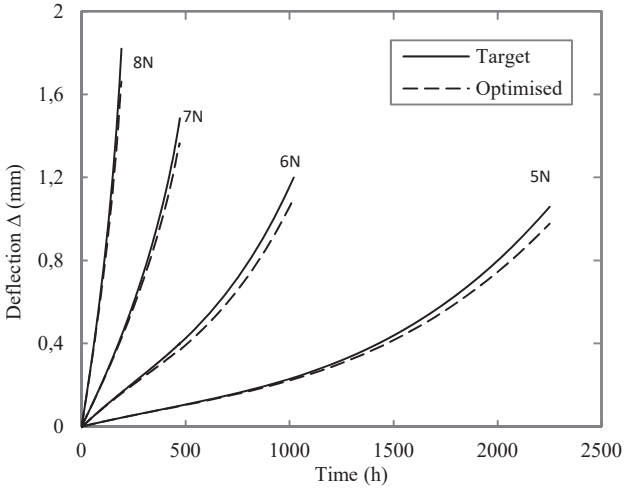


Fig. 6 Deflection curves obtained from the virtue TPB tests and the optimisation procedure for a range of loading

TABLE II
THE MATERIAL PROPERTIES OF THE FICTIONAL MATERIALS M1 AND M2

Material	E	A	n	B	χ	ϕ
M1	150GPa	5×10^{-24}	11	2×10^{-22}	11	5
M2	180GPa	5×10^{-25}	10	2×10^{-24}	10	4.5

To demonstrate the application of the proposed inverse method, it was applied to the two-material system at three different loads, 44N, 46N and 48N. The materials properties of M1 and M2 shown in Table II were used to produce three "theoretical" compound creep stress-strain curves (equivalent to the experimental compound creep responses shown in Fig. 8) as the targets of the optimisation, in which the material M2 was treated as an unknown material. Fig. 9 shows the compound strain-time curves obtained from the optimised creep damage properties compared to the corresponding theoretical experiments. It can be seen that the optimised results agree very well with the target curves for all three different loading forces regarding the strain, strain rate and the time to failure. To further evaluate the quality of the optimisation, the creep strain-time curves were also generated numerically using the creep properties of M2 and the optimised creep properties for a single-

material tensile creep model with three different loading forces: 75N, 80N and 85N. The comparison is shown in Fig. 10. It can be seen that the agreement is still very good, i.e. the strains during the steady-state creep stage are very close for the material M2 and the optimised material at all three loading forces. Although the deviation increases as the creep develops near to failure, the predicted time to failure are close to the target curves. This indicates that the optimised creep properties are capable of giving good prediction of the creep responses of the unknown material at various loading forces, even for the loading cases totally different from the ones in which the optimised properties are obtained.

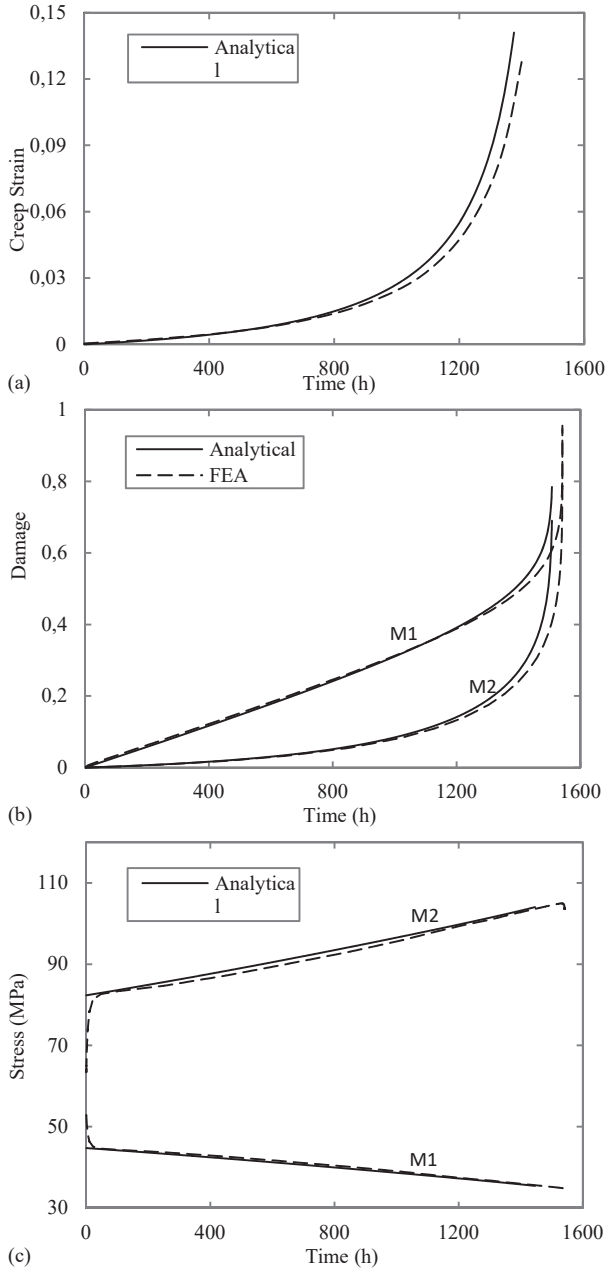


Fig. 7 Forward creep analysis for two-material system (M1 and M2) under the load of 42N: (a) creep strain (b) creep damage and (c) stress

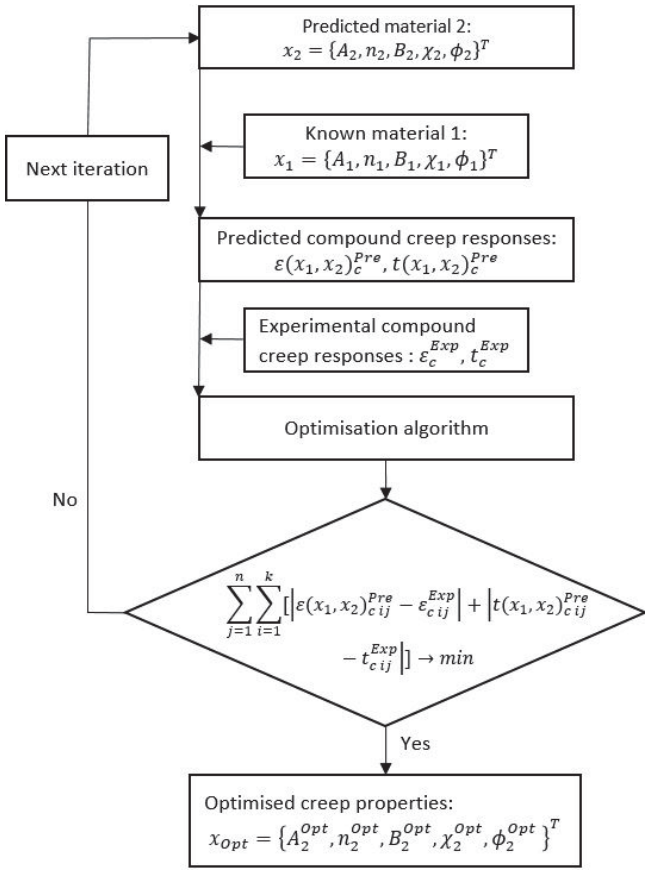


Fig. 8 Flowchart of the inverse method for the two-material case

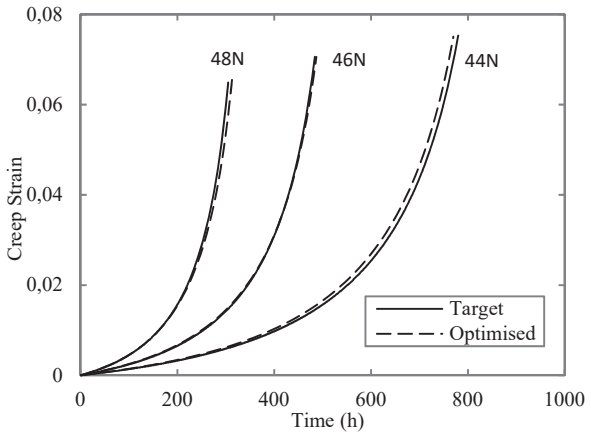


Fig. 9 The optimised curves obtained from the two-material system using the inverse method and the corresponding target curves

V. Discussion And Future Work

Miniature specimen creep testing can be applied in industry to help determine the remaining service life of a component operating at elevated temperature. For this purpose, a method of interpreting test results is required, and this needs an underlying mathematical model of the creep behaviour.

Open Science Index, Materials and Metallurgical Engineering Vol:12, No:10, 2018 publications.waset.org/10009661/pdf

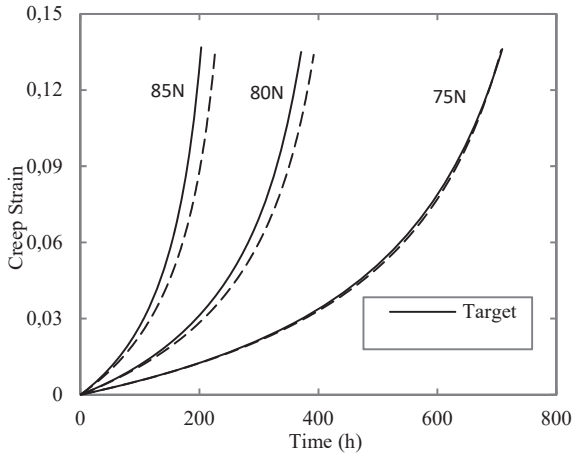


Fig. 10 The single-material model computations for the target material M2 and the optimised creep properties

This paper presents a methodology study which can be used to determine the full stage creep behaviour using the data obtained from miniature specimen creep tests. A three point bending thin beam specimen and a two-material tensile thin plate specimen are used to illustrate the approach. Here, the Kachanov-Rabotnov creep damage model is used to represent the full creep behaviour, and the associated mathematical expressions for the time-dependent load-direction deflection of the three-point bending specimen and strains and damage in the two-material specimen are presented. Analytical solutions are evaluated by the corresponding FE analysis, and excellent comparison is achieved. On this basis, an inverse procedure is used to obtain the creep and damage constants in the Kachanov-Rabotnoy model. The outputs of these equations are iterated numerically using MATLAB codes for various loads. The capability of the optimisation process is demonstrated by the results based on the computed virtue (experimental) tests. The use of analytical solution avoids the need for carrying out FE analysis within the inverse process.

Further validation of the method developed would require experimental testing to be performed. In addition, the two-material formulation could be derived for the TPB situation. For the two-material tensile specimen, sandwich type of configuration may be used to avoid the possibility of bending. Using the experimental data with the inverse method would potentially allow the derived model to be employed in industrial situations to predict the remaining creep life.

Acknowledgment

This work was supported by the Engineering and Physical Sciences Research Council (EPSRC) through EPSRC Centre for Doctoral Training in Innovative Metal Process (IMPaCT, www.impact.ac.uk) [Grant Number EPL016206] and the project "Novel High Temperature Steam Transfer Pipes" [Grant number: EP-R000859-1].

References

[1] T. H. Hyde, W. Sun and J. A. Williams, "The requirements for and the use of miniature test specimens to provide mechanical and creep properties of materials: - a review," *Int. Mater. Rev.,* vol. 52, no. 4, pp. 213-255, 2007.

[2] A. Morris, B.Cacciapuoti and W. Sun, "The role of small specimen creep testing within a life assessment framework for high temperature power plant," Int. Mats. Rev., vol. 63, no. 2, pp. 102-137, 2018.

[3] T. H. Hyde, C. J. Hyde and W. Sun, "A basis for selecting the most appropriate small specimen creep test type," *Trans. ASME J. Pre. Ves. Technol.,* vol. 136, no. 2, pp. 024502-1- 024502-6. 2014.

[4] W. Sun, T. H. Hyde and S. J. Brett, "Application of impression creep data in life assessment of power plant materials at high temperatures," *J. Materials: Design & Applications.,* vol. 222, no.3, pp.175-182, 2008.

[5] W. Sun and T. H. Hyde, "Power plant remaining life assessment using small specimen testing techniques," *9th Annual Conf. on Operational Outages for Power Generation*. 28-30 March, 2011, Amsterdam, The Netherlands.

[6] W. Sun, T. H. Hyde and S. J. Brett, "Small specimen creep testing and application for power plant component remaining life assessment," *4th Int. Conf. on Integrity, Reliability and Failure.* Madeira, 23-27 June, 2013.

[7] T. H. Hyde, W. Sun, A. A. Becker and J. Williams, "Creep properties and failure assessment of new and fully repaired P91 pipe welds at 923 K," *J. Materials: Design and Applications.,* vol. 218, pp. 211-222, 2004.

[8] M. C. Askins and K. D. Marchant, "Estimating the remnant life of boiler pressure parts, EPRI Contract RP2253-1, Part 2, Miniature specimen creep testing in tension," CEGB Report. TPRD/3099/R86, CEGB, UK, 1987.

[9] T. H. Hyde, W. Sun and A. A. Becker, "Analysis of the impression creep test method using a rectangular indenter for determining the creep properties in welds," *Int. J. Mech. Sci*., vol. 38, pp. 1089-1102, 1996.

[10] J. P. Rouse, F. Cortellino, W. Sun, T. H. Hyde and J. Shingledecker, "Small punch creep testing: a review on modelling and data interpretation," *Mater. Sci. Technol*., Vol. 29, no. 11, pp. 1328-1345, 2013.

[11] T. H. Hyde and W. Sun, "A novel, high sensitivity, small specimen creep test," *J. Strain Analysis,* vol. 44, no. 3, pp. 171-185, 2009.

[12] A. Balhassn, T. H. Hyde and W. Sun, "Analysis and design of a small, two-bar creep test specimen," *Trans. ASME J. Eng. Mater. & Technol*., vol. 135 no. 4, pp. 041006-1-041006-9, 2013.

[13] F. Cortellino, J. Rouse, B. Cacciapuoti, W. Sun and T. H. Hyde, "Experimental and numerical analysis of initial plasticity in P91 steel small punch creep samples," *Experimental Mechanics,* vol. 57, no. 8, pp. 1193–1212, 2017.

[14] F.-K. Zhuang, S.-T. Tu, G.-Y. Zhou and Q.-Q. Wang. "Assessment of creep constitutive properties from three-point bending creep test with miniaturized specimens," *J. Strain Analysis,* vol. 46, pp. 1-10, 2014.

[15] Y. Zheng and W. Sun, "An inverse approach for determining creep properties from a miniature thin plate specimen under bending," *Int. J. Mech., Aerospace, Industrial, Machatronic & Manf. Eng.,* vol. 9, no. 7, pp. 1199-1205, 2015.

[16] L. Kachanov, *On rupture time under condition of creep*. Izvestia Akademi Nauk USSR, Otd. Techn. Nauk, Moskwa, 1958, ch. 8, pp. 26-31.

[17] Y. N. Rabotnov *Creep rupture*. 1968. Stanford University: Springer.

[18] J. J. Kang, A. A. Becker and W. Sun, "Determiningelastic–plastic properties from indentation data obtained from finite elementsimulationsandexperimentalresults," *Int. J. Mech. Sci*., vol. 62, pp. 34-46, 2012.

Open Science Index, Materials and Metallurgical Engineering Vol:12, No:10, 2018 publications.waset.org/10009661/pdf